Observing relaxation in device quality InGaN templates by TEM techniques

Cite as: Appl. Phys. Lett. 116, 102104 (2020); https://doi.org/10.1063/1.5139269 Submitted: 18 November 2019 . Accepted: 04 March 2020 . Published Online: 13 March 2020

Tim B. Eldred , Mostafa Abdelhamid , J. G. Reynolds, N. A. El-Masry, James M. LeBeau, and S. M. Bedair







ARTICLES YOU MAY BE INTERESTED IN

Development of microLED

Applied Physics Letters 116, 100502 (2020); https://doi.org/10.1063/1.5145201

Growth of strain-relaxed InGaN on micrometer-sized patterned compliant GaN pseudosubstrates

Applied Physics Letters 116, 111101 (2020); https://doi.org/10.1063/5.0001480

A unified model for vertical doped and polarized superjunction GaN devices Applied Physics Letters 116, 102103 (2020); https://doi.org/10.1063/1.5142855

Lock-in Amplifiers up to 600 MHz







Observing relaxation in device quality InGaN templates by TEM techniques

Cite as: Appl. Phys. Lett. **116**, 102104 (2020); doi: 10.1063/1.5139269 Submitted: 18 November 2019 · Accepted: 4 March 2020 · Published Online: 13 March 2020







Tim B. Eldred, 1 to Mostafa Abdelhamid, 2, a) to J. G. Reynolds, N. A. El-Masry, James M. LeBeau, and S. M. Bedair 2

AFFILIATIONS

- Department of Materials Science and Engineering, North Carolina State University, Raleigh, North Carolina 27695, USA
- ²Department of Electrical and Computer Engineering, North Carolina State University, Raleigh, North Carolina 27695, USA

ABSTRACT

Device quality InGaN templates are synthesized using the semibulk (SB) approach. The approach maintains the film's 2D growth and avoids the formation of indium-metal inclusions. The strain relaxation processes of the grown $In_xGa_{1-x}N$ templates are accompanied by variations in the indium content (x) and lattice parameters (a and c) across the InGaN template's thickness as the residual strain is continuously decreasing. This strain and lattice parameters' variation creates difficulties in applying standard x-ray Diffraction (XRD) and Reciprocal Space mapping (RSM) techniques to estimate the residual strain and the degree of the elastic strain relaxation. We used high-resolution High-angle annular dark-field scanning transmission electron microscopy and Energy-dispersive x-ray spectroscopy (EDS) to monitor the variations of the indium content, lattice parameters, and strain relaxation across the growing $In_xGa_{1-x}N$ templates. We show that strain relaxation takes place by V-pit defect formation. Some of these V-pits are refilled by the GaN interlayers in the $In_xGa_{1-x}N$ SB templates, while others propagate to the template surface. We present an alternative approach combining photoluminescence (PL) and EDS for estimating the degree of strain relaxation in these $In_xGa_{1-x}N$ templates. The values obtained for the degree of relaxation estimated from TEM studies and PL measurements are within reasonable agreement in this study. Device quality $In_xGa_{1-x}N$ templates with $x \sim 0.08$, with a degree of relaxation higher than 70%, are achieved.

Published under license by AIP Publishing. https://doi.org/10.1063/1.5139269

The development of long wavelength III-Nitride Light emitting diodes (LEDs) based on ($In_xGa_{1-x}N/GaN$) multiple quantum wells (MQWs) grown on GaN is typically hindered by the reduced quantum efficiency of the LEDs as the indium content (x) in the wells is increased to achieve the required long wavelength. This reduction in efficiency is attributed to the large lattice mismatch between GaN and InN (11%), which results in high compressive strain on the InGaN QWs.¹ This strain induces a large piezoelectric (PZ) field in the active region of the device, which causes the separation of the electron and hole wavefunctions, resulting in low recombination probability, and hence reduced quantum efficiency.² This strain and PZ field along with the relatively poor InGaN film quality for a high indium content required for green and red emission are believed to be the main cause for the "green gap."^{3,4}

To tackle the green gap problem, the strain in the InGaN MQWs needs to be reduced or eliminated by reducing the lattice mismatch between the MQWs and the underlying template. Relaxed ${\rm In}_x{\rm Ga}_{1-x}{\rm N}$ templates with the indium content close to that of the MQWs represent the optimum solution to alleviate strain. However, such templates are

still not available because of the challenges that exist in growing good quality relaxed bulk InGaN films^{3,5} that are free from V-shaped pits and indium-metal clusters and have atomically smooth surfaces^{5,6} suitable as templates for high indium content MQWs. Several groups have reported different approaches to reduce strain in MQWs such as graded InGaN buffer layers,^{7–9} using ScAlMgO₄ substrates,¹⁰ pseudo InGaN templates separated from GaN films using the smart cut, and wafer bonding approach.¹¹ These approaches, however, are limited to either the low indium content in the $In_xGa_{1-x}N$ template or poor film properties. Thus, In, Ga_{1-v}N QWs with a high indium content needed for green and red emission are highly strained to these templates. Others have reported using an (InGaN/GaN) superlattice (SL) between the GaN buffer layer and the MQWs. 12-14 However, the SL has a low indium content and the InGaN layers are only a few nm thick; hence, the SL is fully strained to GaN and does not relieve the strain in the MQWs albeit the device performance is improved by enhanced electron injection. Another merit of strain reduction in the QWs is that it results in higher indium incorporation in the wells compared to those grown on GaN. 11-15 Thus, using InGaN templates allows for the growth of

a) Author to whom correspondence should be addressed: mabdelh2@ncsu.edu

QWs at higher temperatures, relative to those grown on GaN, generating better quality films for the same indium content in the QWs.

In this work, we present our efforts to achieve relaxed ${\rm In}_x{\rm Ga}_{1-x}{\rm N}$ templates and to investigate the relaxation processes across these templates where (0.06 \leq x \leq 0.12) based on the semibulk (SB) approach. The SB templates are composed of several periods of (InGaN/GaN) layers grown on a thick GaN buffer, where each InGaN sublayer is capped by a GaN interlayer (\sim 1–2 nm thick). The InGaN/GaN period is then repeated multiple times to achieve the desired thickness for a partially or fully relaxed InGaN template. The advantage of the GaN interlayers is to backfill the V-pits generated in the InGaN film as it relaxes. The GaN interlayer also incorporates segregated indium metal clusters at the surface of the growing InGaN film to accomplish a single phase InGaN template. Previous preliminary efforts in developing InGaN templates using the semibulk (SB) approach were reported by our group and others. ^{15–19}

Strain relaxation in InGaN templates is the primary goal toward achieving relaxed InGaN templates. However, strain relaxation is accompanied by a high density of defects. There are several suggested mechanisms for strain relaxation in the bulk InGaN hexagonal wurtzite films including formation of stacking faults, dislocation inclination during growth, inclusion of cubic crystal structures as 3D growth, and V-pit formation. 3.5,6,8,20,21 Therefore, understanding the relaxation processes is important for further development of relaxed InGaN templates.

In the current study, we investigated several growth parameters that affect the relaxation process and film quality of InGaN templates. TEM and EDS are used to follow changes in the indium content (x), lattice parameter "a," and degree of relaxation across the SB grown film. We will demonstrate that relaxation occurs primarily through V-pit formation and that these V-pits are refilled or partially filled by the GaN interlayers during the semibulk growth. Photoluminescence (PL) optical techniques along with EDS were also used to estimate the degree of relaxation of the topmost InGaN templates.

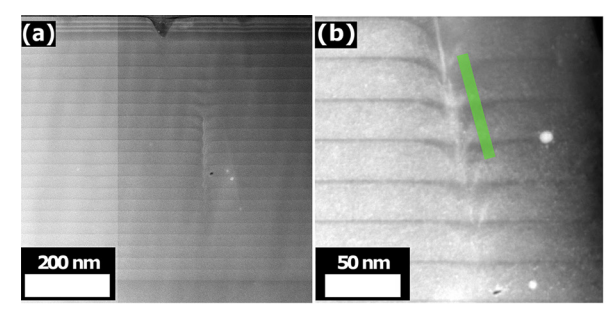
All semibulk (SB) templates were grown on (0001) sapphire substrates by Metal Organic Chemical Vapor Deposition (MOCVD) at 350 Torr with precursors of trimethylgallium (TMGa) and trimethylindium (TMIn) in a hydrogen and nitrogen ambient for group III-elements. The GaN nucleation layer was followed by 2 μ m of intrinsic GaN and 2 μ m of n-type GaN. The reactor temperature was then reduced to grow the In_xGa_{1-x}N layer, 20–35 nm thick, followed by a 1–2 nm interlayer of GaN. The indium content was controlled by varying the growth temperature as has been presented elsewhere. ^{15–17}

Three SB samples grown with 20 periods were investigated. The first SB was intended to have x = 0.08 (8%SB) and 27 nm period thickness estimated from the reactor growth parameters, and then it was capped with three MQWs. The second SB has the same indium

content and period thickness as the first but without the MQWs to be investigated by itself. The third SB was intended to have $x\,{=}\,0.12$ (12%SB) and 33 nm period.

High-resolution x-ray diffraction (HRXRD) was used to determine the SB periodicity. Growth surfaces were characterized by atomic force microscopy (AFM). Optical emission of the SB templates was evaluated by photoluminescence (PL) using a 325 nm He-Cd laser. Samples were prepared for electron microscopy using the silicon stacking method²² paired with wedge polishing using an Allied High Tech Multi-prep system. Argon ion milling was used as a final thinning step. A probe-corrected FEI-Titan S/TEM was operated at 200 kV and used for atomic resolution imaging and strain measurements through the thickness of the film. The probe semi-convergence angle was 19.6 mrad and the collection inner semi-angle for the high-angle annular dark-field scanning transmission electron microscopy (HAADF-STEM) images was 77 mrad. The RevSTEM method was used to correct for sample drift during the acquiring $20\,1024 \times 1024$ frames with a probe dwell time of 3 μ s.²³ A Thermo Fisher Scientific Talos F200X S/TEM operated at 200 kV was used for energy dispersive x-ray spectroscopy (EDS). Thermo Fisher Scientific Velox software was used to measure the wells' composition. The probe semi-angle was 19.6 mrad and drift correction was applied throughout each acquisition. Using Vegard's Law and the indium content measured using EDS for each InGaN layer, the relaxed a lattice parameter was calculated for each layer. The atomic resolution HAADF images of the SB layers were analyzed using 2D Gaussian fitting to locate peak positions, and the lattice parameters averaged over the layer.²⁴ Values were calculated with respect to bulk GaN from the Epi layer. By averaging the lattice parameters over a minimum of 500 data points per layer, the standard error was minimized to allow conclusions to be drawn from the data. The average a-parameter measured from HAADF-STEM images was then used to determine the strain at each InGaN layer, and the degree of relaxation was calculated across the sample.

Figure 1(a) shows the TEM of the 8%SB template capped with three quantum wells. The SB shows consistent flat growth for the InGaN/GaN layers across 20-periods. Each InGaN period is $\sim\!27\,\mathrm{nm}$ thick; the GaN interlayers were intended to be 1.5 nm thick and show minor irregularities in the $\pm0.5\,\mathrm{nm}$ range. Figure 1(b) shows HAADF-STEM data demonstrating the decrease in the indium content as a V-pit is formed along a dislocation and back filled with the GaN interlayers. Figure 1(c) shows EDS along the line profile in Fig. 1(b) demonstrating an increase in Ga-content and a decrease in In-content as the V-pits are backfilled with the GaN interlayers. The period thicknesses of 27 nm for sample 8%SB and 33 nm for sample 12%SB were confirmed using HRXRD (0 0 0 2) scans.



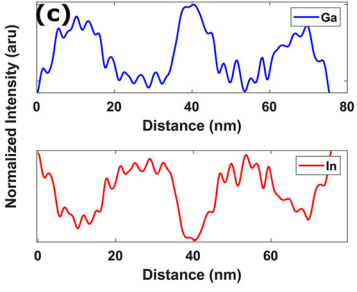
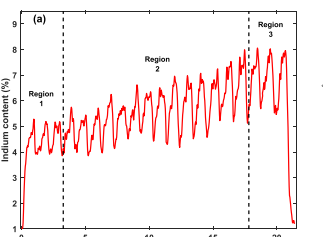
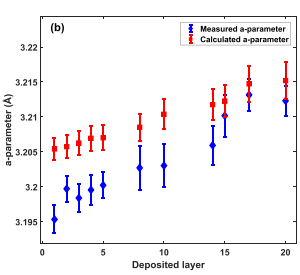


FIG. 1. (a) HAADF-STEM of sample 8% SB, showing a consistent flat growth of InGaN Layers. (b) HAADF-STEM of a dislocation, showing back-filling of the generated V-pits. (c) EDS along the line profile in (b) showing the backfill of the V-pits demonstrates an increase in the Ga content with a decrease in In.





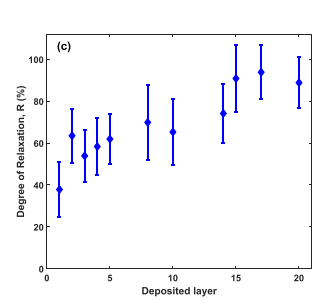


FIG. 2. (a) EDS measurement of 8% SB showing the gradual variation of indium content across the depth of the sample. (b) Lattice parameter "a" measured using HAADF-STEM data, compared to the calculated relaxed lattice parameter using Vegard's law for indium content determined from the EDS data. (c) Degree of relaxation as a function of the deposited layer using the measured and calculated lattice parameters.

To investigate the relaxation mechanism of 8%SB, EDS was performed to estimate the indium content across the film as shown in Fig. 2(a). The atomic fractions were calculated using estimated k-factors for indium and gallium, leading to an estimated 10%-20% relative uncertainty. Results indicate an increase in indium incorporation in each successive InGaN layer. The SB has a varying indium content that starts from $x \sim 0.05$ at the SB/GaN substrate interface to $x \sim 0.08$ at the top 20th period. These values were in good agreement with the SIMS data obtained for this sample. EDS data show that the SB sample has three regions. The first region, close to the GaN substrate, has nearly constant indium content. In the second region, the indium content increases gradually as number of periods increase. In the third region, the indium content levels off at a constant value. The width of these regions depends on the growth conditions of the SB. Notably, the transition between these regions corresponds to the observed relaxation across the InGaN layers. Furthermore, also shown previously, strain and growth mode can play a critical role in determining the shape of the non-abrupt indium concentration found in each layer. 25,26 Using prior measured lattice data, we estimated the degree of relaxation across the 8%SB sample, reported in Fig. 2(b). In this figure, we also used Vegard's law to calculate the lattice parameters for relaxed InGaN for each of the indium content values obtained from EDS using $a_{GaN}=3.1892$ Å, $a_{InN}=3.538$ Å, and bowing parameter $b_{InGaN}=0.003$ Å. To account for the fluctuations in the indium content measured by EDS in each InGaN/GaN period, the EDS data were averaged over a range of 20 points for each InGaN layer of the 20 periods of the SB and then an uncertainty of $\pm 10\%$ was used in the calculations to produce the error bars shown in Fig. 2(b). The calculated a-parameter was then compared with the measured one. The in-plane strain in the grown film decreases with increasing film thickness as shown in Figs. 2(b) and 2(c). The value of "a" obtained experimentally increases gradually and is close to that of fully relaxed InGaN at the topmost layer with the indium content of $x \sim 0.075$ indicating a high degree of relaxation. The degree of relaxation (R) across the

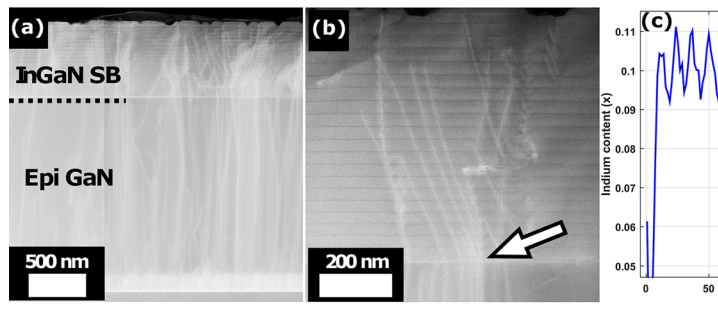
8%SB sample was deduced from the indium content measured by EDS and the corresponding "a" data in Fig. 2(b) using 28

$$R = \frac{a_{InGaN}^{measured} - a_{GaN}}{a_{InGaN}^{relaxed} - a_{GaN}}.$$
 (1)

The results are shown in Fig. 2(c). From the figure, ${\sim}85\%$ relaxed InGaN template with x ${\sim}$ 0.075 is achieved. The error bars account for the error in the degree of relaxation due to uncertainty in the EDS measurement and the accuracy of the measured lattice constants. In addition, the InGaN/GaN interfaces were examined with the atomic resolution HAADF-STEM, and flat surfaces were noted for each layer with the exception of the V-pit regions.

STEM data for sample 12%SB are shown in Fig. 3. The InGaN regions are shown with higher intensity due to the Z-Contrast sensitivity of HAADF-STEM imaging. The sample has a period of 33 nm in agreement with period obtained from HRXRD (0 0 0 2) scan. The indium content across the film was determined using SIMS measurement showing a similar trend to the EDS data of sample 8%SB. The SIMS data in Fig. 3(c) show that the indium content of 12%SB starts at $x \sim 0.08$, and then gradually increases with growing periods until reaching x \sim 0.11 at the topmost period. Our preliminary TEM studies for 8%SB and 12%SB show that the dominant source of dislocations in the film is the dislocations formed at the GaN/sapphire interface. Most dislocations shift direction at the SB/GaN interface as labeled by the arrow in Fig. 3(b), while fewer shift direction further in the SB stack, due to strain. The high density of dislocations, on the order of magnitude of 109 cm⁻², form at the GaN sapphire interface due to the nonoptimum growth conditions of the low temperature GaN buffer layer.

Figures 1 and 3 illuminate the mechanism taking place during the growth and relaxation processes of SB templates as follows. The first several periods are strained to the GaN substrate. This strain is a consequence of the stored strain energy in the SB template not being large enough to initiate relaxation by the formation of V-pits or misfit



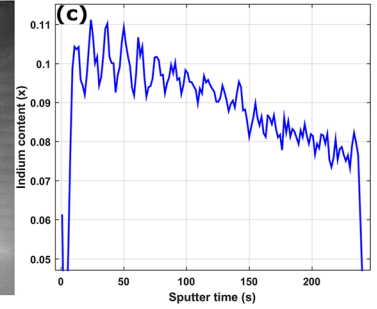


FIG. 3. (a) HAADF-STEM demonstrating the propagation of threading dislocations from the Epi GaN through the 12% semibulk. (b) Demonstrating the deflection of dislocation direction at the interfaces of InGaN-GaN. (c) SIMS Depth profile of sample 12%SB showing the gradual increase in the indium content in the growth direction.

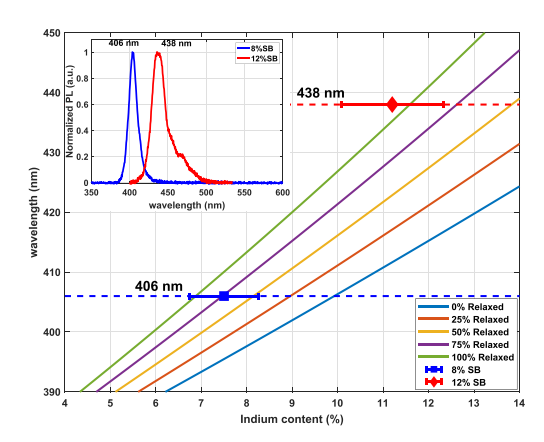


FIG. 4. Wavelength vs indium content for different values of strain. The inset shows normalized PL measurements for both samples 8%SB and 12% SB.

dislocations. Midway through this structure, though, V-pits start to appear along the track of several threading dislocations as shown in Figs. 1(b) and 3(b). These V-pits are backfilled with GaN during the growth of the interlayers. The V-pits are varying in size initially about 60 nm wide and 10-20 nm deep. Since these open hexagonal inverted pyramids are defined by six (10-11) planes, they are deeper and wider as they get closer to the surface. The back filling is a result of the higher growth rate of GaN on the pit facets as compared to that in the (0001) growth direction. In layers where the V-pit does not fully backfill, InGaN growth is slowed by reduced Ga incorporation on the pyramid walls.²⁰ Details of V-pit filling by the GaN interlayers are clearly observed in Fig. 1, the GaN interlayers have darker contrast than InGaN films. The composition of the interlayers is verified by EDS as shown by line profile results in in Fig. 1(c). The V-pits within the SB are filled with GaN; however, as the V-pits get wider and deeper, only partial V-pit filling was achieved as shown at the top V-pit in Fig. 1(a). The process of pits formation and back filling continues until the SB template surface is reached as shown in Fig. 1.

The observed gradual relaxation process shown in Fig. 2 can impact results achieved from the different characterization techniques traditionally used to address degree of strain relaxation. For example, the x-ray reciprocal space mapping (RSM-XRD) technique has a penetration depth of several micrometers. Thus, RSM data for SB templates reflect the variations in the lattice parameters across the entire SB film, resulting in a broad reflection that shows both a high intensity peak for the bottom strained layers with low indium content and a less intense peak for the more relaxed topmost layers with higher indium content. 15 On the other hand, PL technique uses a He-Cd laser with a penetration depth less than 100 nm. Thus, the PL signal can be attributed to emission resulting from the topmost relaxed layers and can be used to estimate the degree of relaxation of the topmost layers for a given indium content, whereas RSM-XRD data represent more of an average across the $\sim 0.5 \mu m$ SB template. The degree of relaxation of the topmost layers in these templates is the factor that influences the strain state in the MQWs when these SB templates are used as substrates.

The inset in Fig. 4 shows the PL emission spectra from the 8%SB without MQW and 12%SB emitting at 406 and 438 nm, respectively. The longer emission wavelength from 12%SB is a result of the higher indium content. In order to estimate the degree of relaxation from PL

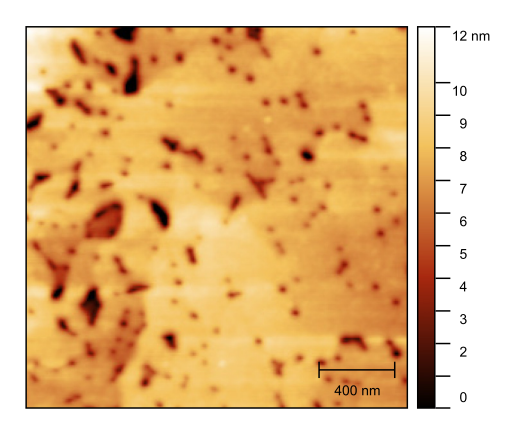


FIG. 5. AFM image of 2 \times 2 $\mu \rm{m}^2$ 8%SB without an MQW structure on it showing a RMS roughness of 1.3 nm.

data, we compared the PL emission with the reported bandgap data for strained and relaxed InGaN by Parker *et al.*²⁹ The model, shown in Fig. 4, was developed¹⁵ using Parker's data to predict the degrees of relaxation (residual strain) from the PL wavelength for a given indium content (x). From the EDS data in Fig. 2(a), the indium content of the top layers for 8%SB has an average of x = 0.075 with a $\pm 10\%$ uncertainty; using this indium content with Fig. 4, the 406 nm emission corresponds to a degree of relaxation of ($\sim 50\% - 100\%$) with a mean of 75%. For 12%SB, SIMS data in Fig. 3(c) show a maximum indium content of $x = 0.112 \pm 0.011$ for the topmost periods; using this indium content with the 438 nm emission corresponds to a degree of relaxation of ($\sim 80\% - 100\%$), practically fully relaxed as shown in Fig. 4.

The AFM micrograph for an 8% SB without MQWs grown on top of it, shown in Fig. 5, reveals an RMS roughness of about 1.3 nm. Thus, from the above results, an InGaN template ($\sim 0.5 \mu m$) with x ~ 0.08 is $\sim 70\%$ relaxed has low surface roughness and is ready as a substrate for further epitaxial growth of nearly lattice matched structures. An AFM micrograph for 12%SB showed RMS roughness of 6.5 nm. Therefore, more work is under way to optimize the growth of higher indium content SB templates with smoother surfaces.

In summary, we used the semibulk approach to synthesize device quality InGaN templates. The approach relies on the growth of thick \sim 25 nm InGaN followed by 1 nm GaN interlayer. The approach maintains the 2D growth, avoids the formation of indium metal inclusions, and enhances the refilling of the V-pit defects. TEM, EDS, and high-resolution STEM were used to monitor the variations of the indium content and lattice parameter "a" across the grown InGaN templates. These data were used to calculate the degree of relaxation across the InGaN templates, showing a variation from \sim 30 to \sim 85% from the bottom layers to the topmost layers. We also show that strain relaxation takes place by V-pit defect formation and with minimal formation of new dislocations. Some of these V-pits are refilled by the GaN interlayers, while others propagate to the template surface and result in surface pits. PL was used as a non-destructive substitute for measuring the degree of relaxation. The PL emission wavelength, for a given value of (x), can be correlated with the bandgap and, thus, the strain in the film. The degree of strain relaxation estimated from STEM studies and PL measurements is within reasonable agreement in these preliminary results. Device quality InGaN templates with $x \sim 0.08$ with a relaxation of $\sim 70\%$ are achieved.

We wish to acknowledge the support of National Science Foundation Grants Nos. ECCS-1407772, ECCS-1665211, and ECCS-1833323. This work made use of instrumentation at AIF acquired with support from the National Science Foundation (No. DMR-1726294). The AIF is a member of the North Carolina Research Triangle Nanotechnology Network (RTNN), a site in the National Nanotechnology Coordinated Infrastructure (NNCI).

REFERENCES

- ¹M. J. Reed, N. A. El-Masry, C. A. Parker, J. C. Roberts, and S. M. Bedair, "Critical layer thickness determination of GaN/InGaN/GaN double heterostructures," Appl. Phys. Lett. 77, 4121–4123 (2000).
- ²P. T. Barletta, E. Acar Berkman, B. F. Moody, N. A. El-Masry, A. M. Emara, M. J. Reed, and S. M. Bedair, "Development of green, yellow, and amber light emitting diodes using InGaN multiple quantum well structures," Appl. Phys. Lett. 90, 151109 (2007).
- ³Z. Liliental-Weber, M. Benamara, J. Washburn, J. Z. Domagala, J. Bak-Misiuk, E. L. Piner, J. C. Roberts, and S. M. Bedair, "Relaxation of InGaN thin layers observed by x-ray and transmission electron microscopy studies," J. Electron. Mater. 30, 439–444 (2001).
- ⁴S. Saito, R. Hashimoto, J. Hwang, and S. Nunoue, "InGaN light-emitting diodes on c-face sapphire substrates in green gap spectral range," Appl. Phys. Express 6, 111004 (2013).
- ⁵Z. Liliental-Weber, D. F. Ogletree, K. M. Yu, M. Hawkridge, J. Z. Domagala, J. Bak-Misiuk, A. E. Berman, A. Emara, and S. Bedair, "Structural defects and cathodoluminescence of In_xGa_{1-x}N layers," Phys. Status Solidi C 8, 2248–2250 (2011).
- ⁶Z. Liliental-Weber, K. M. Yu, M. Hawkridge, S. Bedair, A. Berman, A. Emara, D. R. Khanal, J. Wu, J. Domagala, and J. Bak-Misiuk, "Structural perfection of InGaN layers and its relation to photoluminescence," Phys. Status Solidi C 6, 2626–2631 (2009).
- ⁷J. Däubler, T. Passow, R. Aidam, K. Köhler, L. Kirste, M. Kunzer, and J. Wagner, "Long wavelength emitting GaInN quantum wells on metamorphic GaInN buffer layers with enlarged in-plane lattice parameter," Appl. Phys. Lett. 105, 111111 (2014).
- ⁸K. Hestroffer, F. Wu, H. Li, C. Lund, S. Keller, J. S. Speck, and U. K. Mishra, "Relaxed c-plane InGaN layers for the growth of strain-reduced InGaN quantum wells," Semicond. Sci. Technol. 30, 105015 (2015).
- ⁹T. L. Song, S. J. Chua, E. A. Fitzgerald, P. Chen, and S. Tripathy, "Characterization of graded InGaN/GaN epilayers grown on sapphire," J. Vac. Sci. Technol., A 22, 287–292 (2004).
- ¹⁰T. Ozaki, Y. Takagi, J. Nishinaka, M. Funato, and Y. Kawakami, "Metalorganic vapor phase epitaxy of GaN and lattice-matched InGaN on ScAlMgO₄(0001) substrates," Appl. Phys. Express 7, 091001 (2014).
- ¹¹A. Even, G. Laval, O. Ledoux, P. Ferret, D. Sotta, E. Guiot, F. Levy, I. C. Robin, and A. Dussaigne, "Enhanced in incorporation in full InGaN heterostructure grown on relayed InGaN pseudo-substrate" Appl. Phys. Lett. 110, 262103 (2017).
- grown on relaxed InGaN pseudo-substrate," Appl. Phys. Lett. 110, 262103 (2017).

 W. Lundin, A. Nikolaev, A. Sakharov, E. Zavarin, G. Valkovskiy, M. Yagovkina, S. Usov, N. Kryzhanovskaya, V. Sizov, P. Brunkov, A. Zakgeim, A. Cherniakov, N. Cherkashin, M. Hytch, E. Yakovlev, D. Bazarevskiy, M. Rozhavskaya, and A. Tsatsulnikov, "Single quantum well deep-green LEDs with buried InGaN/GaN short-period superlattice," in 15th International Conference on Metalorganic Vapor Phase Epitaxy (ICMOVPE-XV) [J. Cryst. Growth 315, 267–271 (2011)].
- ¹³N. Nanhui, W. Huaibing, L. Jianping, L. Naixin, X. Yanhui, H. Jun, D. Jun, and S. Guangdi, "Enhanced luminescence of InGaN/GaN multiple quantum wells by strain reduction," Solid-State Electron. 51, 860–864 (2007).

- ¹⁴P.-C. Tsai, Y.-K. Su, W.-R. Chen, and C.-Y. Huang, "Enhanced luminescence efficiency of InGaN/GaN multiple quantum wells by a strain relief layer and proper Si doping," Jpn. J. Appl. Phys., Part 1 49, 04DG07 (2010).
- ¹⁵M. Abdelhamid, J. Reynolds, N. El-Masry, and S. Bedair, "Growth and characterization of ${\rm In_XGa_{1-x}N}$ (0 < x < 0.16) templates for controlled emissions from MQW," J. Cryst. Growth **520**, 18–26 (2019).
- ¹⁶D. M. Van Den Broeck, D. Bharrat, A. M. Hosalli, N. A. El-Masry, and S. M. Bedair, "Strain-balanced InGaN/GaN multiple quantum wells," Appl. Phys. Lett. 105, 031107 (2014).
- ¹⁷D. Van Den Broeck, D. Bharrat, Z. Liu, N. El-Masry, and S. Bedair, "Growth and characterization of high-quality, relaxed $In_yGa_{1-y}N$ templates for optoelectronic applications," J. Electron. Mater. **44**, 4161–4166 (2015).
- ¹⁸K. Pantzas, Y. E. Gmili, J. Dickerson, S. Gautier, L. Largeau, O. Mauguin, G. Patriarche, S. Suresh, T. Moudakir, C. Bishop, A. Ahaitouf, T. Rivera, C. Tanguy, P. Voss, and A. Ougazzaden, "Semibulk InGaN: A novel approach for thick, single phase, epitaxial InGaN layers grown by MOVPE," in 16th International Conference on Metalorganic Vapor Phase Epitaxy [J. Cryst. Growth 370, 57–62 (2013)].
- ¹⁹S. Alam, S. Sundaram, M. Elouneg-Jamroz, X. Li, Y. E. Gmili, I. C. Robin, P. L. Voss, J.-P. Salvestrini, and A. Ougazzaden, "InGaN/InGaN multiple-quantum-well grown on InGaN/GaN semi-bulk buffer for blue to cyan emission with improved optical emission and efficiency droop," Superlattices Microstruct. 104, 291–297 (2017).
- ²⁰X. H. Wu, C. R. Elsass, A. Abare, M. Mack, S. Keller, P. M. Petroff, S. P. DenBaars, J. S. Speck, and S. J. Rosner, "Structural origin of V-defects and correlation with localized excitonic centers in InGaN/GaN multiple quantum wells," Appl. Phys. Lett. 72, 692–694 (1998).
- ²¹A. V. Lobanova, A. L. Kolesnikova, A. E. Romanov, S. Y. Karpov, M. E. Rudinsky, and E. V. Yakovlev, "Mechanism of stress relaxation in (0001) InGaN/GaN via formation of V-shaped dislocation half-loops," Appl. Phys. Lett. 103, 152106 (2013).
- 22J. Dycus and J. Lebeau, "A reliable approach to prepare brittle semiconducting materials for cross-sectional transmission electron microscopy," J. Microscopy 268, 225–229 (2017).
- 23X. Sang and J. M. LeBeau, "Revolving scanning transmission electron microscopy: Correcting sample drift distortion without prior knowledge," Ultramicroscopy 138, 28–35 (2014).
- ²⁴X. Sang, A. A. Oni, and J. M. LeBeau, "Atom column indexing: Atomic resolution image analysis through a matrix representation," Microsc. Microanal. 20, 1764–1771 (2014).
- ²⁵K. Muraki, S. Fukatsu, Y. Shiraki, and R. Ito, "Surface segregation of in atoms during molecular beam epitaxy and its influence on the energy levels in InGaAs/GaAs quantum wells," Appl. Phys. Lett. 61, 557–559 (1992).
- ²⁶J. Houston Dycus, S. Washiyama, T. B. Eldred, Y. Guan, R. Kirste, S. Mita, Z. Sitar, R. Collazo, and J. M. LeBeau, "The role of transient surface morphology on composition control in AlGaN layers and wells," Appl. Phys. Lett. 114, 031602 (2019).
- ²⁷J. Piprek, Nitride Semiconductor Devices: Principles and Simulation (Wiley Online Library, 2007), Vol. 590.
- ²⁸M. Schuster, P. O. Gervais, B. Jobst, W. Hösler, R. Averbeck, H. Riechert, A. Iberl, and R. Stömmer, "Determination of the chemical composition of distorted InGaN/GaN heterostructures from x-ray diffraction data," J. Phys. D: Appl. Phys. 32, A56–A60 (1999).
- ²⁹C. A. Parker, J. C. Roberts, S. M. Bedair, M. J. Reed, S. X. Liu, N. A. El-Masry, and L. H. Robins, "Optical band gap dependence on composition and thickness of $In_xGa_{1-x}N$ (0 < x < 0.25) grown on GaN," Appl. Phys. Lett. **75**, 2566–2568 (1999).